

1 **Low-altitude Measurements of 2-6 MeV Electron Trapping Lifetimes at  $1.5 \leq L \leq 2.5$**

2 D.N. Baker and S.G. Kanekal

3 *Laboratory for Atmospheric and Space Physics, 1234 Innovation Drive, Boulder, CO 80303-*  
4 *7814*

5

6 R.B. Horne, N.P. Meredith, and S.A. Glauert

7 *British Antarctic Survey, Madingley Road, Cambridge, CB3 0ET, United Kingdom*

8

9 Abstract

10

11 During the Halloween Storm period (October-November 2003), a new Van Allen belt electron  
12 population was powerfully accelerated. The inner belt of electrons formed in this process de-  
13 cayed over a period of days to years. We have examined quantitatively the decay rates for elec-  
14 trons seen in the region of  $1.5 \leq L \leq 2.5$  using SAMPEX satellite observations. At  $L=1.5$  the e-  
15 folding lifetime for 2-6 MeV electrons was  $\tau \sim 180$  days. On the other hand, for the half-dozen  
16 distinct acceleration (or enhancement) events seen during late-2003 through 2005 at  $L \sim 2.0$ , the  
17 lifetimes ranged from  $\tau \sim 8$  days to  $\tau \sim 35$  days. We compare these loss rates to those expected from  
18 prior studies. We find that lifetimes at  $L=2.0$  are much shorter than the average 100-200 days  
19 that present theoretical estimates would suggest for the overall  $L=2$  electron population. Addi-  
20 tional wave-particle interaction aspects must be included in theoretical treatments and we de-  
21 scribe such possibilities here.

22

23 Introduction

24 Radiation belt electron loss processes are relatively poorly understood. It is clear that adia-  
25 batic changes resulting from the gradual buildup of the ring current (Kim and Chan, 1997), as  
26 well as magnetopause shadowing of closed electron drift paths (Wilken et al., 1986; Shprits et  
27 al., 2006a), are insufficient to account for the observed losses throughout most of the trapping  
28 region. Currently, the most promising mechanism for MeV electron loss is VLF wave scattering

29 (Lorentzen et al., 2001) into the loss cone. Although field line stretching probably plays a role in  
30 the local time dependence of loss (Onsager et al., 2002; Green et al., 2004) at higher L-values,  
31 recent evidence suggests that wave scattering may be the most important overall loss process  
32 (Millan and Thorne, 2007).

33 It is significant that the L-shell of the maximum outer radiation belt flux correlates well with  
34 the statistical location of the plasmapause as a function of Dst (e.g., Li et al., 2006). This sug-  
35 gests that the cold plasma density in the plasmasphere plays an important role in controlling the  
36 L-dependent inward penetration of the outer radiation belts. While progress has been made in  
37 understanding the action of some loss processes and their consequences for controlling outer ra-  
38 diation belt morphology, in-situ measurements from throughout the inner magnetosphere are  
39 critical to the development of an understanding of how radiation belt particles are lost (Meredith  
40 et al., 2006). This paper utilizes such an approach.

41 Interior to the plasmapause, a variety of waves contribute to electron decay rates (Abel and  
42 Thorne, 1998). These include whistler-mode waves from plasmaspheric hiss, from lightning, and  
43 from ground-based transmitters that leak out into the magnetosphere. Just outside the plasma-  
44 pause, chorus is thought to produce electron microburst precipitation (Lorentzen et al., 2001) and  
45 other electron scattering (Shprits et al., 2007). The competition between acceleration and loss  
46 over an extended region near the plasmapause must be resolved in order to understand electron  
47 dynamics in the heart of the radiation belts. The plasmapause often resides in the region near 5  
48  $R_E$ . However, during disturbed times it typically moves to lower L. The plasmapause moves  
49 within 3.5  $R_E$  approximately 5-40 times per year, depending on the specific solar cycle, with  
50 more than 20 occurrences in most years (based on model calculations). During the 2003 Hallow-

51 een storm the plasmapause was displaced inside  $2 R_E$  and remained at this compressed location  
52 for several days (Baker et al., 2004).

53 As will be described in this paper, the 2003 Halloween Storm was a remarkable “active” ex-  
54 periment performed by nature. It produced a “new” radiation belt inside the magnetosphere  
55 (Baker et al., 2004), caused by wave acceleration by whistler mode chorus (Horne et al., 2005;  
56 Shprits et al., 2006b) which could then be observed to decay over the subsequent days and  
57 weeks. The powerful storm that occurred just three weeks after the Halloween Storm (on 20 No-  
58 vember 2003) produced a distinctive set of electron acceleration and loss processes that have  
59 been studied previously in some detail (Bortnik et al., 2006).

60 In the present paper we examine several specific acceleration, or enhancement, events that  
61 were observed after the 2003 Halloween Storm period during the years 2003-2005. We focus on  
62 the range  $1.5 \leq L \leq 2.5$  in the inner magnetosphere and we determine empirical electron lifetimes  
63 by observing flux decay timescales. These lifetimes are compared and contrasted with prior re-  
64 sults and theoretical expectations.

65

## 66 1. Data Selection

67 The primary data set used in this paper is the E=2-6 MeV electron channel of the Solar,  
68 Anomalous, and Magnetospheric Particle Explorer (SAMPEX) Proton/Electron Telescope (PET)  
69 experiment (see Baker et al., 1993). SAMPEX operates in a roughly circular 600-km altitude,  
70  $82^\circ$ -inclination orbit. For the present study, we use daily averages of electron data sorted accord-  
71 ing to magnetic L-shells. The L-values correspond roughly to the geocentric radial distance in  
72 Earth radii ( $1 R_E = 6372$  km) that a magnetic field line crosses the equatorial plane. L-values are  
73 determined using the IGRF magnetic field model. It is recognized that for higher L-values (e.g.,

74  $L \geq 5.0$ ), there can be significant distortion away from a dipole configuration. Here we focus on  
75 relatively low  $L$ -values where the IGRF approximation is quite good.

76 In order to place SAMPEX particle measurements into context, we have also used upstream  
77 solar wind data from the Advanced Composition Explorer (ACE) spacecraft and ground-based  
78 geomagnetic information (such as  $K_p$  and  $Dst$ ). These data show that the events analyzed here  
79 are associated with significant geomagnetic storms. However, the principal point is specifically  
80 to examine inner zone and radiation belt slot region enhancements in their own right, irrespective  
81 of ring current, solar wind, or other geomagnetic variations.

82 It is recognized that low-altitude measurements of electron fluxes may be subject to some  
83 ambiguity in timing as compared to measurements near the magnetic equator. However, the “re-  
84 markable coherence” seen between near-equatorial platforms and the low-altitude SAMPEX  
85 measurements (e.g., Kanekal et al., 2001) suggests that this is not generally a severe problem.  
86 We therefore start with the assumption that the lifetimes derived from SAMPEX data are indica-  
87 tive of the inner zone and slot-region relativistic electron populations as a whole.

88

## 89 2. Observations

90 Figure 1 summarizes solar wind speed and relativistic electron (2-6 MeV) intensities for the  
91 years 2003 through 2005, inclusive. Fig. 1a shows daily averages of the solar wind speed meas-  
92 ured by ACE sensors. The dashed horizontal line at  $V_{sw}=500$  km/s emphasizes the widely-  
93 recognized fact that solar wind speeds above this level almost always “drive” relativistic electron  
94 production throughout the outer radiation zone (e.g., Baker et al., 1998).  $V_{sw}$  was, on average,  
95 above 500 km/s for most of 2003 and for the early part of 2004, due to the presence of recurrent

96 high-speed solar wind streams. For the latter part of 2004, the solar wind speed was quite low  
97 and throughout 2005, the value of  $V_{sw}$  was mixed.

98 Figure 1b shows a color-coded representation of the 2-6 MeV electron flux measured by the  
99 SAMPEX PET sensors. The vertical scale shows L-values and the horizontal scale is time (in  
100 Day of Year [DOY], measured from the beginning of 2003). The logarithm of the directional  
101 flux of 2-6 MeV electrons is shown by color as indicated by the color bar to the right of the fig-  
102 ure.

103 As would be expected based on the high solar wind speeds in 2003, the overall radiation belt  
104 population was persistently elevated from DOY 1 through DOY~500, or so. Through the latter  
105 part of 2004 and for much of 2005 (DOY~500 to DOY~850) the electron intensities were often  
106 quite low for  $3 \leq L \leq 8$ . Notable exceptions were seen at DOY~580 (July 2004) and DOY~680  
107 (November 2004) when powerful storms occurred,  $V_{sw}$  increased dramatically, and major relativ-  
108 istic electron events were initiated.

109 One of the most striking features seen in Fig. 1b was the slot-filling event and the creation of  
110 a “new” population of relativistic electrons in the inner zone ( $1.0 \leq L \leq 2.0$ ) in association with  
111 the 2003 Halloween Storm period (Baker et al., 2004). This belt of electrons appeared rather  
112 suddenly on DOY~305 and persisted through the end of 2005 (i.e., DOY~1100). The inner zone  
113 belt of electrons was seen to be enhanced by several of the storms (DOY=580, DOY=680, etc.  
114 that were noted in the previous paragraph.

115 In order to better time and quantify the electron flux increases at various L-values, we have  
116 taken “cuts” in L from L=1.5 to L=2.2. These flux values for each L are shown by the different  
117 colored lines in Fig. 2. This representation shows that the Halloween Storms enhanced the elec-  
118 tron flux at L=1.5 by a factor of ~50 or more. This inner zone flux then remained very elevated

119 to the end of 2005 (decaying gradually over time). On the other hand, the flux values at  $L=2.0 \pm$   
120  $0.2$  increased by as much as five orders-of-magnitude and then decayed quite rapidly in each  
121 case back to pre-Halloween values. At least 5 electron enhancement events can be easily identi-  
122 fied following the large October-November 2003 event.

123

### 124 3. Analysis and Interpretation

125 The abrupt rises and more gradual decays of electron fluxes seen in several events in Fig. 2  
126 suggest that we can make empirical determinations of electron lifetimes assuming the fluxes to  
127 decay exponentially. We have performed such analyses for the six distinct enhancement-decay  
128 episodes seen from November 2003 through the end of 2005 by performing least-squares fits for  
129 each decay interval to obtain life times.

130 Figure 3 shows detailed examples for three of the intervals. Figure 3a is for the Halloween  
131 Storm (and, in addition, the 20 November 2003 storm, since their effects were commingled). The  
132 red curve shows the flux profile for  $L=1.5$ , while the blue curve shows the  $L=2.0$  profile. The  
133 black dashed lines show exponential decay (least-squares) fits to the data trends. At  $L=1.5$ , we  
134 find that  $J=Ke^{-t/\tau}$  with  $\tau \sim 180$  days. (This same decay rate applies for essentially all of the  $L=1.5$   
135 data through the end of 2005). For the  $L=2.0$  data we have specifically fit the data points for  $305$   
136  $\leq \text{DOY} \leq 410$ . This fit gives  $\tau=18.6$  days. Note that from  $\text{DOY} \sim 410$  to  $\text{DOY} \sim 560$ , the decay rate  
137 was slower with a decay lifetime in excess of 30 days. Thus, the apparent electron lifetimes de-  
138 pend on the length of interval chosen for analysis. We have typically examined periods of  $\sim 100$   
139 day duration.

140 Fig. 3b shows the next major storm enhancement event that commenced on  $\text{DOY} \sim 570$  ( $\sim 23$   
141 July 2004). This corresponded to a complex, multi-step geomagnetic storm that reached  $\text{Dst} \sim -$

142 200 nT. We have fit the decay of this event at  $L=2.0$  for the period  $575 \leq \text{DOY} \leq 675$  and find  
143  $\tau=13.4$  days. As a final illustrative example, a much weaker event that commenced about  
144  $\text{DOY}=970$  (late August 2005) is shown in Fig. 3c. For this event we find a much more gradual  
145 decay. For the interval  $970 \leq \text{DOY} \leq 1090$ , we find  $\tau = 26.5$  days.

146 Table 1 shows the six intervals analyzed and the e-folding times for each interval at  $L=2.0$ .  
147 As noted previously, for  $L=1.5$  a steady value of  $\tau \sim 180\text{d}$  describes the decay throughout the en-  
148 tire period of time, aside from small bump-ups of flux associated with the major storms. On av-  
149 erage for  $L=2.0$ , we find a decay rate for all events to be  $\langle \tau \rangle = 20.2\text{d} \pm 8.7$ . This is short com-  
150 pared to previous theoretical estimates (e.g., Abel and Thorne, 1998).

151

#### 152 4. Summary and Discussion

153 To summarize our key findings we note that:

- 154 1. The Halloween 2003 storms produced a ‘new’ inner zone relativistic (2-6 MeV) electron  
155 belt that persisted for years at  $L \sim 1.5$ .
- 156 2. The gradual decay of the new belt was highly  $L$ -dependent:
  - 157 • At  $L=1.5$ , the decay was seen to be  $J=K \exp(-t/\tau)$  with  $\tau \sim 180\text{d}$ .
  - 158 • At  $L=2.0$ , the decay exhibited  $\tau \sim 18\text{d}$ .
- 159 3. Several subsequent storms in 2004-2005 produced clear flux enhancements  
160 in the inner zone (6 events were readily identified).
- 161 4. The decay of the  $L=1.5$  population continued throughout; the  $L=2.0$  popu-  
162 lations decayed with  $7.9 \leq \tau \leq 34.8\text{d}$ .

163 5. Theoretical estimates suggest that  $\tau$ -values at  $L=2.0$  and  $E=2$  MeV should  
164 be  $\tau \sim 100$ d due to plasmaspheric hiss.

165 The specifications of electron decay lifetimes are complicated due to the fact that there are  
166 several competing wave-particle interaction mechanisms that can be operative. Inside the plas-  
167 masphere, losses are mostly due to scattering caused by plasmaspheric hiss waves, by magneto-  
168 spherically-reflecting (MR) whistler waves, and by coulomb collisions (Abel and Thorne, 1998).  
169 Such loss had previously been estimated to lead to characteristic lifetimes of  $\sim 100$  days at  $E \sim 1.5$   
170 MeV energies. There were expected to be strong  $L$ - and energy-dependences. The Abel and  
171 Thorne (1998) calculations included the effects of losses due to VLF transmitters as well as hiss,  
172 MR whistlers, and Coulomb collisions. The assumptions made concerning VLF transmitters  
173 could be a source of discrepancy between observations and models.

174 Outside the plasmasphere, chorus emissions would produce very fast pitch angle scattering  
175 leading to lifetimes of order one day or less (Horne et al., 2005; Albert, 2005). Electromagnetic  
176 ion cyclotron (EMIC) waves can possibly provide even faster losses of electrons with  $E > 500$   
177 keV (Summers and Thorne, 2003). Some estimates for EMIC losses – although quite localized  
178 spatially – would give lifetimes of just hours. However, these waves need frequencies with high  
179 values of  $f_{pe}/f_{ce}$  to resonate with  $\sim 2$  MeV electrons. The ratio of  $f_{pe}/f_{ce}$  tends to become smaller as  
180 one goes to lower  $L$  inside the plasmapause (e.g., from 4 to 2). Thus, the EMIC waves will tend  
181 to resonate with higher energy electrons, which probably become too high for the energies we  
182 observe here. Since these waves are generated by anisotropic proton distributions associated with  
183 the ring current, and the ring current does not usually penetrate to  $L=2$ , it is unclear how they can  
184 be generated near  $L=2$ .



185 For the results reported here, we have focused on the spatial region inside  $L \sim 3.0$  and have  
186 quantitatively assessed loss lifetimes for  $L \sim 1.5-2.0$ . Under most circumstances (other than, say,  
187 the period right after the Halloween Storm), the  $L$ -values examined here would be well within  
188 the plasmasphere. Thus, we would expect the hiss lifetimes to be the applicable ones.

189 As noted in Section 2 above, we believe that our determination of  $L$ -value for SAMPEX data  
190 sorting is relatively accurate. Thus, this should provide a solid basis for theoretical comparison.  
191 We know that the chosen energy channel responds to a broad range of electrons and there could  
192 be some ambiguity in this matter. However, from our analyses (not shown here) we find the en-  
193 ergy spectra around  $L=2.0$  to be strongly falling ( $J=KE^{-\gamma}$ , with  $\gamma \sim 2.5$ ). Thus, the data we have  
194 shown would be dominated by electrons with  $E \sim 2.0$  MeV.

195 In very recent work (Meredith et al., 2007), estimates have been made of electron lifetimes as  
196 a function of energy,  $L$ -value and geomagnetic activity levels. The analyses examine lifetimes  
197 due to hiss, ducted whistlers, and magnetospherically reflecting whistlers. It is found that at  
198  $L=2.0$  and  $E \sim 2$  MeV, the lifetime for electrons would be at least  $\tau \sim 100-200$  days. The  $L$ -  
199 dependence, however, is very strong such that  $\tau$  drops precipitously to 1-10 days at  $L=2.5$ . From  
200 the Meredith et al. (2007) modeling, the lifetime also drops rapidly with increasing energy. Thus,  
201 the experimental results we have presented here (with  $\tau \sim 20$ d) have to be considered in the con-  
202 text of great sensitivity to  $L$  position and the broad range (2-6 MeV) of our analyzed energy  
203 range. We note that the lifetimes of about 100 days in the Meredith et al. (2007) paper assume  
204  $AE^* > 500$ nT during the decay. They are longer for  $AE^* < 100$  nT, particularly for 5 MeV elec-  
205 trons.

206 One possible explanation for the very short apparent electron lifetimes reported here lies in  
207 the fact that plasmaspheric hiss is mainly responsible for the loss of 2-6 MeV electrons at equato-

208 rial pitch angles  $<65^\circ$  at  $L=2$ . Detailed model results show that it takes much longer to scatter  
209 electrons at larger equatorial pitch angles into the loss cone. At  $L=2$  and at 600 km, a  $90^\circ$  pitch  
210 angle particle at SAMPEX corresponds to approximately an  $18^\circ$  particle at the equator in a di-  
211 pole field. In a careful analysis motivated by the present observations, we find that the pitch an-  
212 gle diffusion rates for 2 MeV electrons at  $L=2$  due to plasmaspheric hiss show a deep minimum  
213 for pitch angles greater than  $65^\circ$ . This means that electrons at larger equatorial pitch angles take  
214 much longer to diffuse into the loss cone. This analysis also provides the decay rate of the elec-  
215 tron distribution function at the same energy. The initial condition assumed for the modeling is a  
216 flat pitch angle distribution. The distribution function decays more quickly at small pitch angles  
217 than at  $90^\circ$ , as expected. The timescales for loss at  $18^\circ$  equatorial pitch angle, corresponding to  
218 that which would be observed by SAMPEX, is 23 days, whereas the timescale for the whole dis-  
219 tribution to decay is 284 days (Meredith et al., 2007), assuming quiet magnetic activity (as repre-  
220 sented by  $AE^* < 100$  nT). Thus there is good agreement with the observations presented here for  
221 the particles at pitch angles measured by SAMPEX. At higher L shells ( $L=2.5$  and larger) there is  
222 no deep minimum in the diffusion rates in the model. This would explain why we tend to get  
223 such a high degree of global coherence at higher L values (Kanekal et al., 2001).

224 In a paper in preparation, we pursue the issues raised here and we make more detailed com-  
225 parisons between observations and theoretical models. This continuing work should help further  
226 clarify electron lifetime expectations in this key region of the inner magnetosphere.

227

228 Acknowledgments. This work was supported by grants from NASA and from the National  
229 Science Foundation. We thank Mary Hudson, Scot Elkington, Xinlin Li, and Ian Mann for help-  
230 ful comments and advice on this work.

231

232

232 References

- 233 Abel, B., and R.M. Thorne, Electron scattering loss in Earth's inner magnetosphere, 1, Dominant  
234 physical processes, *J. Geophys. Res.*, *103*, 2385-2396, 1998.
- 235 Albert, J.M., Evaluation of quasi-linear diffusion coefficients for EMIC waves in a multi-species  
236 plasma, *J. Geophys Res.*, *108(A6)*, 1249, doi: 10.1029/2002JA009792, 2003.
- 237 Baker, D.N., et al., An overview of the Solar, Anomalous, and Magnetospheric Particle Explorer  
238 (SAMPEX) mission, *IEEE Trans. Geosci. Remote Sens.*, *31(3)*, 531, 1993.
- 239 Baker, D.N., X. Li, J.B. Blake, and S. Kanekal, Strong electron acceleration in the Earth's mag-  
240 netosphere, *Adv. Space Res.*, *21*, No. 4, 609-613, 1998.
- 241 Baker, D.N., et al., An extreme distortion of the Van Allen belt arising from the 'Hallowe'en' so-  
242 lar storm in 2003, *Nature*, *432*, 878-881, doi:10.1038/nature03116, 2004.
- 243 Bortnik, J., et al., Observation of two distinct, rapid loss mechanisms during the 20 November  
244 2003 radiation belt dropout event, *J. Geophys. Res.*, *111*, A12216, doi:10.1029/  
245 2006JA011802, 2006.
- 246 Green, J.C., et al., Testing loss mechanisms capable of rapidly depleting relativistic electron flux  
247 in the Earth's outer radiation belt, *J. Geophys. Res.*, *109*, A12211, doi:10.1029/  
248 2004JA010579, 2004.
- 249 Horne, R.B., et al., Wave acceleration of electrons in the Van Allen radiation belts, *Nature*, *437*,  
250 227, doi: 10.1038/nature03939, 2005.
- 251 Kanekal, S.G., D.N. Baker, and J.B. Blake, Multi-satellite measurements of relativistic electrons:  
252 Global coherence, *J. Geophys. Res.*, *29*, 721-732, 2001.
- 253 Kim, H.-J., and A.A. Chan, Fully adiabatic changes in storm time relativistic electron fluxes, *J.*  
254 *Geophys. Res.*, *102*, 22, 107, 1997.

255 Li X., D. N. Baker, T. P. O'Brien, L. Xie, Q. G. Zong, Correlation between the inner edge of  
256 outer radiation belt electrons and the innermost plasmopause location, *Geophys. Res. Lett.*,  
257 33, L14107, doi:10.1029/2006GL026294, 2006.

258 Lorentzen, K.R., J.B. Blake, U.S. Inan, and J. Bortnik, Observations of relativistic electron mi-  
259 crobursts in association with VLF chorus, *J. Geophys. Res.*, 106, 6017, 2001.

260 Meredith, N.P., et al., Energetic outer zone electron loss timescales during low geomagnetic ac-  
261 tivity, *J. Geophys. Res.*, 111, A05212, doi:10.1029/2005JA011516, 2006.

262 Meredith, N.P., et al., Slot region electron loss timescales due to plasmaspheric hiss and light-  
263 ning generated whistlers, *J. Geophys. Res.*, in press, 2007.

264 Millan, R.M., and R.M. Thorne, Review of radiation belt relativistic electron losses, *J. Atmos.*  
265 *Solar-Terr. Phys.*, 69, 362-377, 2007.

266 Onsager, T., et al., Radiation belt electron flux dropouts: local time, radial and particle-energy  
267 dependence, *J. Geophys. Res.*, 107(A11), 1382, doi:10.1029/2001JA000187, 2002.

268 Shprits, Y.Y., et al., Outward radial diffusion driven by losses at magnetopause, *J. Geophys.*  
269 *Res.*, 111, A11214, doi: 10.1029/2006JA011657, 2006a.

270 Shprits, Y.Y., et al., Acceleration mechanism responsible for the formation of the new radiation  
271 belt during the 2003 Halloween solar storm, *Geophys. Res. Lett.*, 33, L05104,  
272 doi:10.1029/2005GL024256, 2006b.

273 Shprits, Y.Y., N.P. Meredith, R.M. Thorne, Parameterization of radiation belt electron loss time-  
274 scales due to interactions with chorus waves, *Geophys. Res. Lett.*, 34, L11110,  
275 doi:10.1029/2006GL029050, 2007.

276 Summers, D., and R.M. Thorne, Relativistic electron pitch-angle scattering by electromagnetic  
277 ion cyclotron waves during geomagnetic storms, *J. Geophys. Res.*, 108(A4), 1143,  
278 doi:10.1029/2002JA009489, 2003.

279 Wilken, B., D.N. Baker, P.R. Higbie, T.A. Fritz, W.P. Olson, and K.A. Pfizter, Magneto-  
 280 spheric configuration and energetic particle effects associated with a SSC: A case  
 281 study of the CDAW-6 event on March 22, 1979, *J. Geophys. Res.*, 91, 1459, 1986.

282

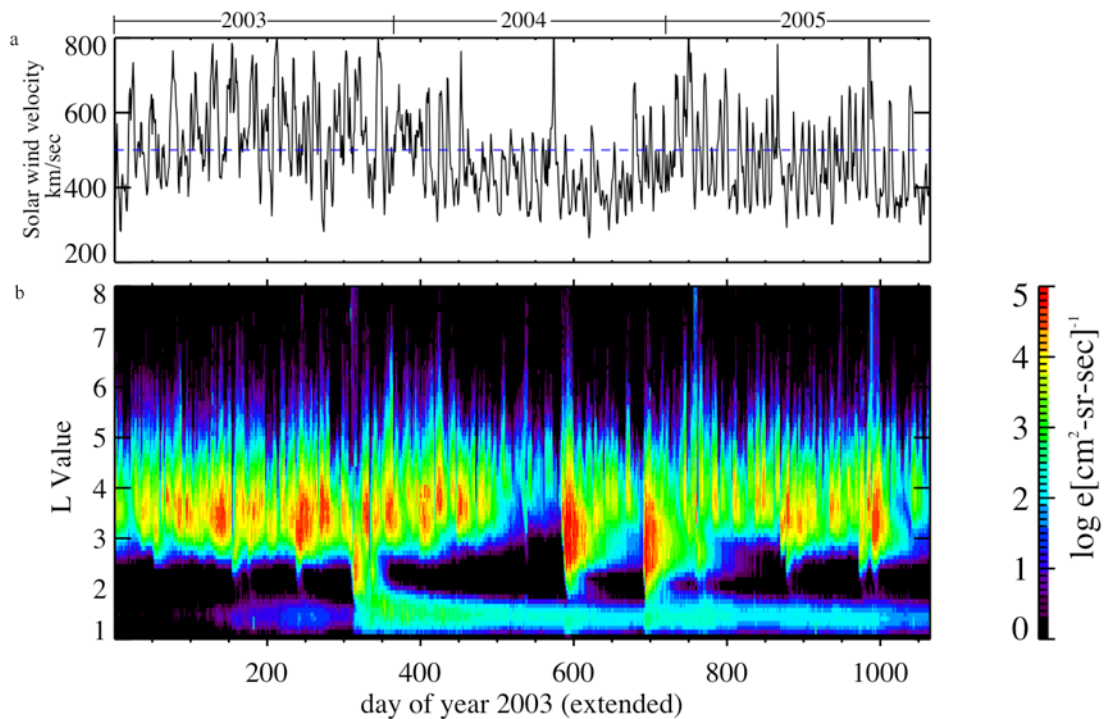
283  
 284

Table 1. Empirical Electron Trapping Lifetimes

2 ≤ E ≤ 6 MeV; L~2.0	
DOY (2003)	e-folding Lifetime (d)
305-410	18.6 ± 1.8
575-675	13.4 ± 1.1
680-720	7.9 ± 0.8
760-860	19.9 ± 2.1
860-970	34.8 ± 3.1
970-1090	26.5 ± 2.3

285  
 286

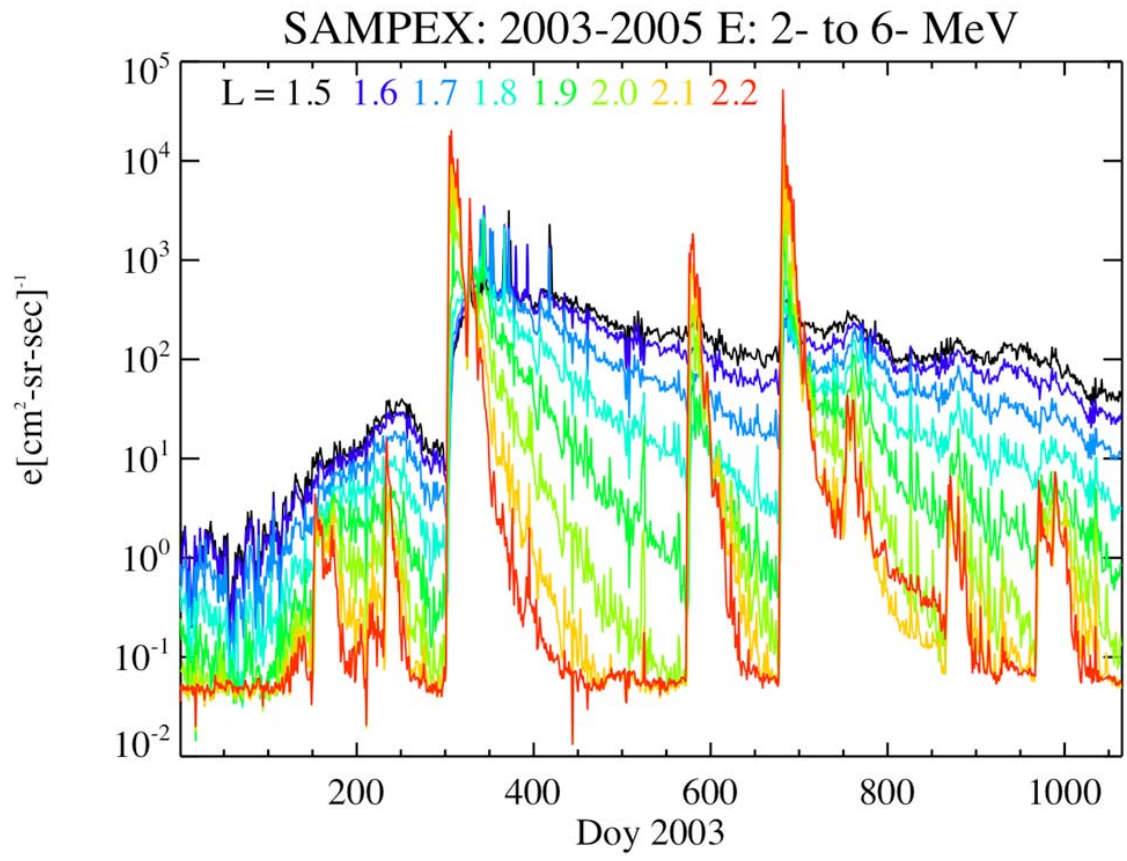
$$\langle \tau \rangle = 20.2d (\pm 8.7)$$



287

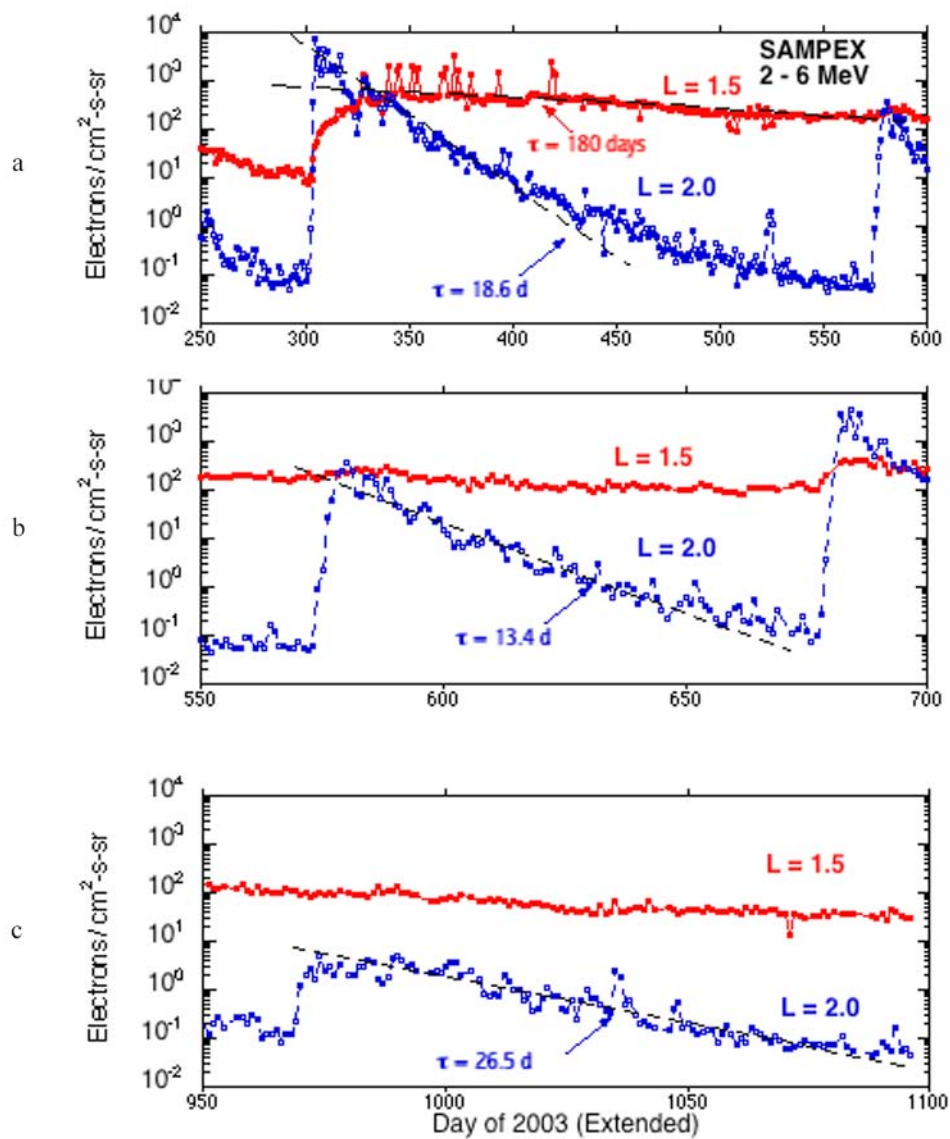
288 Figure 1

289



290

291 Figure 2



292

293 Figure 3

294



294 Figure Captions

295 Fig. 1. Daily-averaged data for the years 2003-2005 inclusive. (a) Solar wind speeds measured  
296 by instruments onboard the ACE spacecraft upstream of the Earth's magnetosphere. (b) Relativ-  
297 istic (2-6 MeV) electron fluxes for the range  $1 \leq L \leq 8$  in a logarithmic color-coded format as  
298 shown by the color bar to the right. Data were obtained from instruments onboard the SAMPEX  
299 spacecraft.

300 Fig. 2. Cuts taken for several different fixed L-values (delineated near the top of the figure) for  
301 the period 2003-2005 inclusive. The vertical axis is directional particle intensity and the horizon-  
302 tal axis is time reckoned in days (Day of Year) from the beginning of 2003. Several flux en-  
303 hancement events are evident.

304 Fig. 3. Details of several electron enhancement events (as seen in Fig. 2). The red curves corre-  
305 spond to fluxes measured at  $L=1.5$ , while the blue curves show measurements at  $L=2.0$ . The  
306 black dashed lines show least-squares empirical fits. (a) Data for DOY 250-600 of 2003 (ex-  
307 tended). (b) Data for DOY 550 – 700 inclusive. (c) Data for DOY 950 – 1096 inclusive.